

EXPERIMENTAL INVESTIGATIONS ON A SURFACE MICROMACHINED TUNABLE LOW PASS FILTER

V. Janardhana¹, S. Pamidighantam², N. Chatteraj¹, J. S. Roy^{3, *}, S. R. Kuppireddi⁴, and R. G. Kulkarni⁵

¹ECE Department, Birla Institute of Technology, Mesra, Ranchi, India

²Center for Emerging Technologies, SBMJCE, Kanakpura, Bangalore Rural, India

³School of Electronics Engineering, KIIT University, Bhubaneswar, Orissa, India

⁴Department of Informatics, University of Oslo, Oslo, Norway

⁵Bharat Electronics Ltd., Jalahalli, Bangalore, India

Abstract—In this paper, a surface micromachined microwave tunable low pass filter, consisting of tunable shunt capacitors and series inductors, has been realized. The filter exhibits insertion loss of less than 1 dB (up to 10 GHz), stop band attenuation of 20 dB at 20 GHz, and cut-off frequency is changed to 8 GHz with the application of DC actuation voltage in the structure. The filter has an overall dimension of 5.5 mm × 2 mm. The characteristics of tunable filter are investigated with and without packaging.

1. INTRODUCTION

Radio frequency microelectromechanical systems (RF MEMS) are suitable for various applications ranging from mobile phones to satellite and terrestrial broadband communications to commercial applications due to their low-power consumption, low loss, and good linearity [1, 2]. RF MEMS devices, such as series switch, shunt switch, micromachined inductor, tunable low pass filter, tunable band pass filter, tunable capacitor and micro-mechanical resonator with

Received 18 August 2011, Accepted 11 November 2011, Scheduled 21 November 2011

* Corresponding author: Jibendu Sekhar Roy (drjsroy@rediffmail.com).

impressive performance characteristics [3–17], are attractive. With their advantages, the RF MEMS tunable filters [4, 8, 13, 16, 17] are of interest as they substantially reduce the size of the analog front-end subsystem for multi-band applications and can dynamically reject large-signal interferers. MEMS technology can be applied in this field to obtain electronically re-programmable filters. An overview of the application of RF MEMS switches in tunable filters is described in [4]. In [8], a new type of reconfigurable inductor is used, together with MEMS capacitive shunt switches, to realize a millimeterwave reconfigurable low pass filter. Several high-performance integrated silver band-pass filters with high out-of-band rejection through the use of inductive parasitic are reported in [13]. Reports are available [16] where metamaterials are used for reconfigurable RF MEMS filters. Some adaptively tunable microstrip band-pass filters are described in [17] for the use in ultra wide band (UWB) system, but the insertion loss seems to be high. There are several good filter topology candidates such as lumped element, comb line, capacitive gap-coupled, direct coupled series etc.

In this paper, two types of tunable low pass filters, Type A and Type B, are fabricated and measured. Optical pictures of the fabricated structures are shown in Figure 1. Characteristics of RF MEMS filters are investigated experimentally, using vector network analyzer with and without packaging, for feasibility study.

These tunable filters are used in scanning receivers. These filters are part of the filter bank, covering a band of frequencies (which are part of RF MEMS integrated circuits).

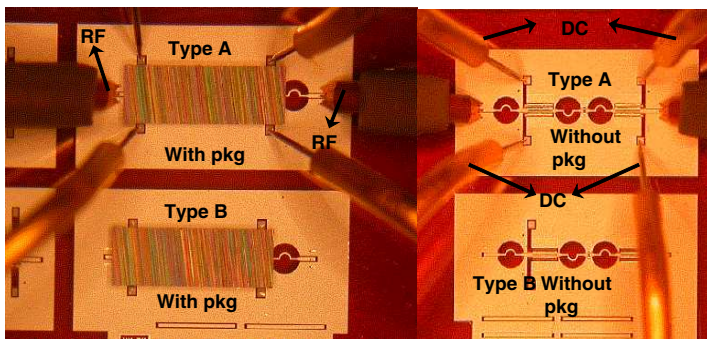


Figure 1. Optical micrograph pictures of low pass filter with and without wafer level package.

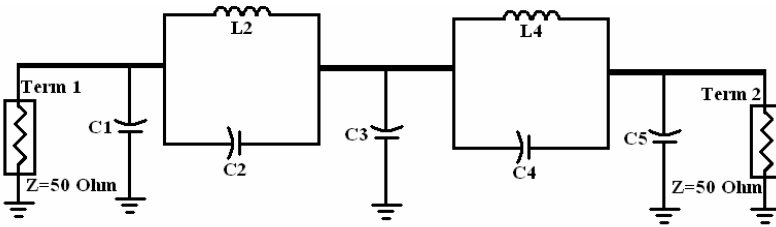


Figure 2. Elliptic low pass filter topology.

2. TECHNOLOGY AND FABRICATION OF MEMS TUNABLE LOW PASS FILTER

In Figure 1, Type A & Type B are same low pass filters, and the only difference is the bias DC pads. Both Type A and Type B have cut-off frequency of 12.5 GHz with DC biasing of 0 Volt with and without packaging. But for Type A, thick metal is used for DC actuation, and for Type B, thin metal is used for DC actuation.

The elliptic low pass filter topology [18] is used in the present MEMS filter structure. The important design parameters of elliptic filters include ripple in the pass band and attenuation in the stop band. Figure 2 is the circuit schematic of elliptic low pass filter with five elements.

In this particular RF MEMS filter, $C1 = 0.33$ pF, $C2 = 0.12$ pF, $C3 = 0.45$ pF, $C4 = 0.42$ pF, $C5 = 0.19$ pF, $L2 = 0.8$ nH and $L4 = 0.43$ nH.

The values of the elements are taken from [18], having a ripple of 0.18 dB in the pass band and roll off angle given by 58° .

The low pass filter, fabricated here, is a fixed beam structure (Figure 3), which is a micro machined capacitive bridge. The variable bridge capacitor is formed between the central conductor & the bridge across the central conductor. The height of the bridge/beam from the central conductor is $3.5 \mu\text{m}$. At the bottom plate, the central conductor is fixed, and at the top plate (movable), bridge/beam is suspended over the bottom plate and fixed at both ends. The bridge/beam is pulled down by electrostatic actuation.

In Figure 3, the dimensions are as follows: $W = 100 \mu\text{m}$, $G = 18 \mu\text{m}$, $S = 10 \mu\text{m}$, $w = 20 \mu\text{m}$. There are 24 bridges in each variable capacitor.

SU-8-10 Packaging scheme is used for packaging (SU-8 is used for the electrical layer, and the clean wafer is then spin-coated with a $10 \mu\text{m}$ thickness, which is SU-8-10), and the effect of the packaging is also shown.

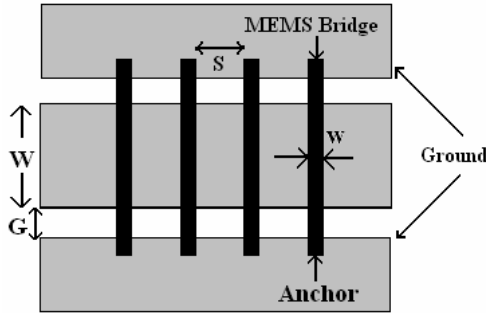


Figure 3. Schematic layout of tunable capacitor.

To build an RF MEMS structure with micromachining, the wafer could be processed using conventional processes to create transmission line capacitors and inductors that are required before the RF MEMS processing starts. A resist layer is then deposited and patterned to protect this part of the circuit from the RF MEMS processing steps. This layer can be removed at the completion of RF MEMS fabrication. The surface micromachining involves the selective adding and removing of metal, dielectric and sacrificial layers on the substrate surface. Depending on the step, either a metal or a dielectric or a sacrificial layer is then deposited, patterned and etched. This sequence of steps is repeated until the required RFMEMS three-dimensional structure is completed. The process employs four masks for device fabrication and one additional mask for the fabrication of package structure. Four inches quartz wafers are used for the device fabrication. The package structures are patterned in the form of rings of SU8-10 on standard silicon substrate. The released structures of tunable low pass filters are subjected to wafer level packaging using chip on wafer bonding with the help of Fine Tech Fine Placer Flip Chip Bonding. Further, the effects of introducing thick metal for DC actuation in the ground plane (Type A in Figure 1) and thin metal for DC actuation (Type B in Figure 1) are studied.

The DC bias pads (running under the bridge/beam) are used for electrostatic actuation. The increase in the actuation voltage is attributed to the gap between bridges/beams & the DC pads. The gap is $3\ \mu\text{m}$ in Type A topology, (using thick pad of $3.5\ \mu\text{m}$) and $6\ \mu\text{m}$ in Type B topology (using thin pad of $0.5\ \mu\text{m}$). Due to different thicknesses of bias pads and different gaps between the bridges/beams and DC pads, in Type A and Type B, pull-in-voltages are different for the two types [2].

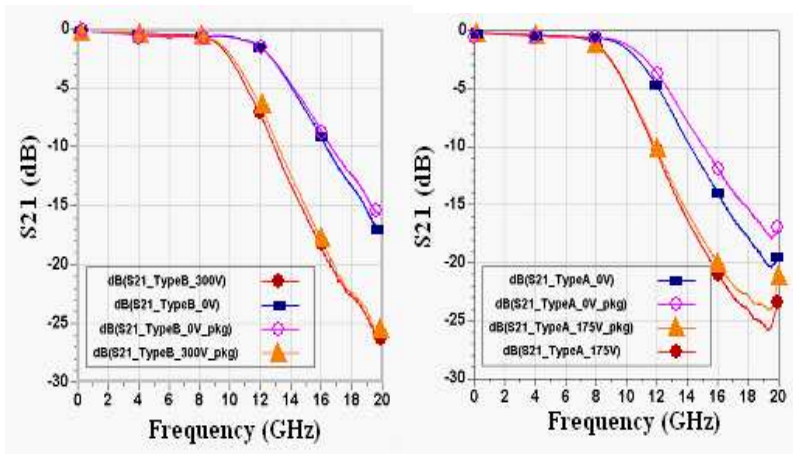


Figure 4. Measured results (S_{21}) for Type A and Type B MEMS tunable filters.

The pull-in-voltage (V_p) for electrostatic actuation is given by [2]

$$V_p = \sqrt{(8kg^3/27\epsilon_0 A)} \quad (1)$$

where, ' g ' is the gap between bridges/beams and DC pads, ' ϵ_0 ' the free space permittivity, ' k ' the spring constant of the bridge/beam, and ' A ' the effective overlap area of the parallel plates.

3. MEASUREMENT AND RESULTS

Vector network analyzer (Agilent PNA 8362B) along with wafer level prober (Cascade Micro Tech RF1 probe station) is used for the characterization. Type A and Type B low pass filters are measured at 0 V DC bias and up to 175 V DC bias. The structures are then subjected to wafer level packaging scheme using SU8-10 packaging technique. The measurements are carried out after packaging. Measured S -parameter results are shown in Figures 4 and 5.

When a DC bias of 175 Volt is applied through DC probes to filter Type A, cut-off frequency reduces to 8 GHz, both with and without packaging. When a DC bias of 300 Volt is applied through DC probes to filter Type B, cut-off frequency reduces to 10 GHz both, with and without packaging. The effect of packaging is minimal. The insertion loss for both types of filters is nearly 1 dB up to 10 GHz.

The capacitor and inductor values, used in Figure 2, are taken from [18], where, the effects of fringing capacitance and slight non

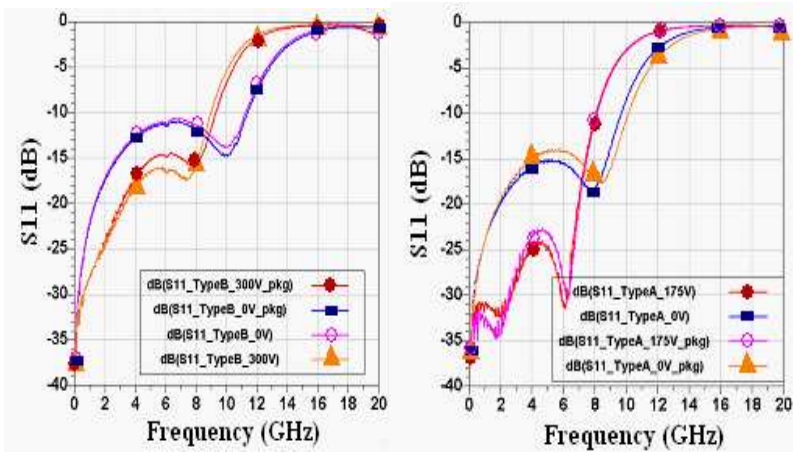


Figure 5. Measured results (S_{11}) for Type A and Type B MEMS tunable filters.

uniformities in the bridge height, due to process variations and hence the change in the capacitance value in fabricated filter, have not been taken into account. The electrical field between the top bridges/beams and the central conductors is no longer straight and would bend at the edges (as the periphery of the bridges/beam is more due to the gaps between bridges/beams), hence the capacitance between the plates is more than the actual one, which is not accounted while calculating the overlap area between plates. This fringing field capacitor would increase the pulling electrostatic voltage and loss of the line. The loss of the line is inversely proportional to the impedance. Again, the loss due to skin effect in fabricated filter is important in the fabricated structure. In this particular structure, the skin depth for gold is $0.747 \mu\text{m}$ at 10 GHz. The center conductor thickness is $3 \mu\text{m}$. Therefore, the loss due to skin effect is negligible.

4. CONCLUSION

Measurements for S -parameters of a fabricated tunable MEMS low pass filter are carried out. From the measured S -parameters, more meaningful parameters such as insertion loss, isolation, etc. can be predicted. Bandwidth of the filter can be tuned by varying the actuation voltage. The fabrication procedure with packaging is described, and it is experimentally found that for both types of fabricated filters, the effect of packaging may be neglected.

ACKNOWLEDGMENT

The authors would like to thank the support provided by the Government of India under the National Program on Smart Materials (NPSM) for this work and also thank BEL, Bangalore, India.

REFERENCES

1. Shang, J. and M. J. Lancaster, *Microwave Filters for RF Applications*, Wiley, 2000.
2. Rebeiz, G. M., *RF MEMS Theory, Design and Technology*, Wiley-Interscience, New York, 2003.
3. Barker, N. S. and G. M. Rebeiz, "Distributed MEMS true-time delay phase shifters and wide band switches," *IEEE Transactions on Microwave Theory and Techniques*, Vol. 46, No. 11, Nov. 1998.
4. Brank, J., J. Yao, M. Eberly, A. Malczewski, K. Varian, and C. Goldsmith, "RF MEMS based tunable filters," *International Journal of RF and Microwave Computer-Aided Engineering*, Vol. 11, No. 5, 276–284, Sep. 2001.
5. Rebeiz, G. M., G. L. T. Tan, and J. S. Hayden, "RF MEMS phase shifters: Design and applications," *IEEE Microwave Magazine*, Vol. 3, 72–81, Jun. 2002.
6. Natarajan, K., B. Sriram, Y. Chandana, K. Chandrasekhar, H. B. Ganapathy, B. Dasan, K. S. Reddy, and S. Pamidighantam, "Overview of MEMS activities at BEL," *Proceedings of the Fourth International Conference on Smart Materials, Structures and Systems*, SE-109–116, Bangalore, India, Jul. 28–30, 2005.
7. Laha, R., B. Sriram, A. T. Kalghatki, K. Natarajan, and S. Pamidighantam, "Design, development and characterization of surface micromachined passive components for radar applications," *Proceedings of International Radar Symposium (IRS)*, Bangalore, India, Dec. 2005.
8. Lee, S., J. Kim, J. Kim, Y. Kim, and Y. Kwon, "Millimeter-wave MEMS tunable low pass filter with reconfigurable series inductors and capacitive shunt switches," *IEEE Microwave and Wireless Components Letters*, Vol. 15, No. 10, 691–693, Oct. 2005.
9. McFeeters, G. and M. Okoniewski, "Distributed MEMS analog phase shifter with enhanced tuning," *IEEE Microwave and Wireless Components Letters*, Vol. 16, No. 1, 34–36, Jan. 2006.
10. Janardhana, V., R. G. Kulkarni, and J. S. Roy, "Feasibility study of MEMS distributed phase shifters for phased array," *International Symposium on Microwaves, ISM*, Dec. 2006.

11. Janardhana, V., J. S. Roy, S. Pamidighantam, and R. G. Kulkarni, "Analysis of surface micro machined RF MEMS phase shifters," *IEEE Aerospace & Electronic Systems Magazine*, Vol. 23, No. 5, 32–35, May 2008.
12. Jahanbakht, M., M. Naser-Moghadasi, and A. A. Lotfi Neyestanak, "Low actuation voltage Ka-band fractal MEMS switch," *Progress In Electromagnetics Research C*, Vol. 5, 83–92, 2008.
13. Shim, Y., R. Tabrizian, F. Ayazi, and M. Rais-Zadeh, "Low-loss MEMS band-pass filters with improved out-of-band rejection by exploiting inductive parasitics," *International Electron. Devices Meeting (IEDM09)*, 801–804, Baltimore, USA, Dec. 7–9, 2009.
14. Topalli, K., M. Unlu, H. I. Atasoy, S. Demir, O. Aydin Civi, and T. Akin, "Empirical formulation of bridge inductance in inductively tuned RF MEMS shunt switches," *Progress In Electromagnetics Research*, Vol. 97, 343–356, 2009.
15. Raedi, Y., S. Nikmehr, and A. Poorziad, "A novel bandwidth enhancement technique for X-band RF MEMS actuated reconfigurable reflectarray," *Progress In Electromagnetics Research*, Vol. 111, 179–196, 2011.
16. Gil, I., M. Morata, R. Fernández-García, X. Rottenberg, and W. De Raedt, "Reconfigurable RF-MEMS metamaterials filters," *PIERS Proceedings*, 1239–1242, Marrakesh, Morocco, Mar. 20–23, 2011.
17. Pillans, B. W., A. Malczewski, F. J. Morris, and R. A. Newstrom, "A family of MEMS tunable filters for advanced RF applications," *IEEE MTT-S International Symposium*, Baltimore, USA, Jun. 5–10, 2011.
18. Glover, I. A., S. R. Pennock, and P. R. Shepherd, *Microwave Devices, Circuits and Subsystems for Communications Engineering*, John Wiley and Sons, 2005.